Journal of Hazardous Materials 185 (2011) 93–100

Contents lists available at ScienceDirect

Journal of Hazardous Materials

journal homepage: www.elsevier.com/locate/jhazmat

Modified native cellulose fibers—A novel efficient adsorbent for both fluoride and arsenic

Ye Tian[a,b], Min Wu[c,*], Ruigang Liu[a], Deqian Wang[a,b], Xiaobo Lin[a,b], Weili Liu[a,b], Lin Ma[a,b], Yanding Li[e], Yong Huang[a,c,d,*]

[a] State Key Laboratory of Polymer Physics and Chemistry, Beijing National Laboratory for Molecular Sciences, Institute of Chemistry, Chinese Academy of Sciences, Beijing, 100190, China
[b] Graduate School, Chinese Academy of Sciences, Beijing, 100039, China
[c] State Engineering Research Center of Engineering Plastics, Technical Institute of Physics and Chemistry, Chinese Academy of Sciences, Beijing, 100190, China
[d] Laboratory of Cellulose and Lignocellulosics Chemistry, Guangzhou Institute of Chemistry, Chinese Academy of Sciences, Guangzhou, 510650, China
[e] East China University of Science and Technology, Shanghai, 200237, China

ARTICLE INFO

Article history:
Received 9 July 2010
Received in revised form 1 September 2010
Accepted 1 September 2010
Available online 9 September 2010

Keywords:
Cellulose fibers
Fluoride
Arsenic
Adsorption
Water treatment

ABSTRACT

Native cellulose fibers were surface modified by poly(*N*,*N*-dimethyl aminoethyl methacrylate) (PDMAEMA) to generate an anion adsorbent, which was characterized by scanning electron microscopy, fourier transform infrared spectroscopy and elemental analyzer. This adsorbent had high efficiency in removal of F^-, AsO_2^- and AsO_4^{3-} from aqueous solutions, even at low initial concentrations. Adsorption kinetics showed that the adsorption equilibrium could be reached within 1 min. The distribution coefficient did not change with adsorbent dose, indicating the adsorption was a homogenous process. Langmuir, Freundlich and Temkin models were used to fit the adsorption isotherms. Based on the parameters calculated from the models, the adsorption capacity was in the order of $AsO_4^{3-} \gg AsO_2^- > F^-$, and the adsorption was a favorable process. Compared with Freundlich and Temkin models, the isotherms followed Langmuir model a little better.

1. Introduction

Fluoride and arsenic pollutions are commonly found in the groundwater on global levels, affecting large populations in Canada, China, United States, Bangladesh, India, Mexico, etc. [1–3]. They both exist in water in the form of anions. Fluoride is an essential component for the dental and bone health of mammals, but as a double-edged sword, the excessive intake of fluoride through food and drink may cause chronic diseases such as mottling of teeth, skeletal fluorosis and neurological damage in severe cases [4,5]. Arsenic, predominantly in the inorganic forms of arsenite (III) and arsenate (V), is primarily introduced into groundwater from oxidative weathering and geochemical reactions [6]. Intake of arsenic can lead to disturbance of the cardiovascular and nervous system functions, and sharply increase risks of cancer in skin, lungs, liver, kidney, and bladder [7]. According to World Health Organization (WHO) [8] norms, the upper limit of concentration in drinking water is 1.0 mg L^{-1} for fluoride and 0.01 mg L^{-1} for arsenic [8].

Many treatment methods for removing fluoride and arsenic have been reported thus far, such as chemical precipitation [9,10], ion exchange [11,12], adsorption [13], membrane [14], electrolysis [15], coagulation [16], and lime treatment [17]. Some of these methods have disadvantages. For example, the cost for ion exchange, electrolysis and membrane processes is usually high, while precipitation, coagulation and lime treatment processes will produce large amounts of toxic sludge, needing further treatments. Among all these methods mentioned above, adsorption has been recognized as an effective technique for treating fluoride and arsenic-contaminated water. Many materials can be used as adsorbents, such as activated carbon [18], chitosan [19,20], alumina [21], calcite [22], fly ash [23], lanthanum-impregnated silica gel [24], and bone char [25,26]. However, some of them are efficient only at high ion concentrations [27], and some of them are really expensive (like activated carbon). In addition, arsenic pollution is often accompanied with fluoride pollution in practical cases. The existing adsorbents can only adsorb arsenic or fluoride separately. Even for the arsenic adsorption, it needs to oxidize As (III) to As (V) at first, and then the latter can be adsorbed [28]. So it is necessary to find an adsorbent that (i) can adsorb both fluoride and arsenic (either arsenite or arsenate) with high efficiency, and (ii) has a low-cost/benefit ratio.

* Corresponding authors.
E-mail address: wumin@mail.ipc.ac.cn (M. Wu).

0304-3894/$ – see front matter © 2010 Elsevier B.V. All rights reserved.
doi:10.1016/j.jhazmat.2010.09.001

Native cellulose, arisen as crystalline microfibrils, constitutes the most abundant and renewable polymer resource available worldwide. Cellulose is inexpensive and abundant in hydroxyl groups, which can attach functional groups through a variety of chemical modifications. If the attached functional groups are amine groups such as $-NH_2$, –NRH, and $-NR_1R_2$, which can be protonated in aqueous solutions to form positive groups like $-NH_3^+$, $-NRH_2^+$, and $-NR_1R_2H^+$, the toxic anions in aqueous solutions can be adsorbed through electrostatic interaction. *N*,*N*-Dimethyl aminoethyl methacrylate (DMAEMA) is a tertiary amine-based monomer and can be polymerized through a variety of reactions, such as atom transfer radical graft polymerization [29] and reversible addition-fragmentation chain transfer polymerization [30]. In this work, we used native cellulose fibers as template, and grafted poly(*N*,*N*-dimethyl aminoethyl methacrylate) (PDMAEMA) onto its surface. These modified cellulose fibers were presented as effective adsorbents for removing F^-, AsO_2^- and AsO_4^{3-} from aqueous solutions. The characteristics of the adsorption behavior were studied under equilibrium and dynamic conditions. This work can be extended to prepare adsorbents by making use of agro- or plant-residues.

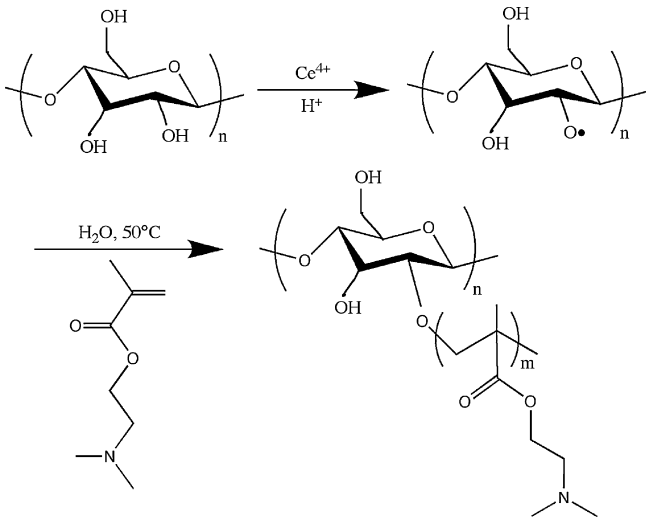

Scheme 1. Synthetic route for the cellulose-g-PDMAEMA.

2. Experimental

2.1. Materials

Cellulose fibers were prepared via grinding the native cellulose cardboard by a grinder. The obtained cellulose fibers were washed with deionized water, methanol and acetone, and then vacuum dried. The monomer *N*,*N*-dimethyl aminoethyl methacrylate (DMAEMA, Aldrich) was purified by vacuum distillation. The initiator ammonium cerium (IV) nitrate ($(NH_4)_2Ce(NO_3)_6$, Alfa Aesar) was used without further purification. Nitric acid (65–68 wt%), sodium fluoride (NaF), sodium arsenite ($NaAsO_2$) and sodium arsenite dibasic ($Na_2HAsO_4{\cdot}7H_2O$) were all analytical grade supplied by local chemical agent suppliers and were used as received. Potassium nitrate from Alfa Aesar was used without further treatment. Sodium chloride (NaCl), sodium sulfate (Na_2SO_4) and sodium hydrogen carbonate ($NaHCO_3$) were all analytical grade supplied by local chemical works and used as received, offering competing anions.

2.2. Synthesis of cellulose-g-PDMAEMA

Ceric ion (Ce^{4+}) initiated polymerization [31,32] was used to graft PDMAEMA onto the cellulose fiber surface, as shown in Scheme 1. About 0.5 g of cellulose fibers were dispersed in 42 mL of 4.34×10^{-2} mol L^{-1} $(NH_4)_2Ce(NO_3)_6$ aqueous solution with 0.69 mol L^{-1} HNO_3. The solution was purged with nitrogen for 30 min before 3 mL DMAEMA was added drop wise. After another 10 min of nitrogen purging, the solution was heated under magnetic stirring at 50 °C for 3 h. Then the PDMAEMA grafted cellulose fibers were rinsed in deionized water for several times and dried in vacuo.

2.3. Fluoride and arsenic adsorption

In this study, the solutions of F^-, AsO_2^-, and AsO_4^{3-} were obtained respectively from sodium fluoride (NaF), sodium arsenite ($NaAsO_2$) and sodium arsenite dibasic ($Na_2HAsO_4{\cdot}7H_2O$). The effects of initial ion concentration, initial pH value, adsorbent dose and the existence of other anions on the equilibrium adsorption capacity were taken into consideration. The adsorption isotherms and kinetics were also studied. For the adsorption capacity tests, cellulose-g-PDMAEMA was magnetic stirred in aqueous anion solutions with a known concentration. The adsorption capacity q (mg g^{-1}) was calculated from the following expression:

$$q = \frac{(C_0 - C_f)V}{m} \quad (1)$$

where C_0 and C_f represent the initial and final concentrations of the anion solutions, respectively. V and m are the solution volume and adsorbent mass, respectively. The adsorbent dose (m/V) was kept 1 g L^{-1} for all the experiments except the adsorbent dose study.

2.4. Characterization

The morphology of the cellulose fibers was studied using a JSM-6700F field emission scanning electron microscopy (FE-SEM). A TENSOR 27 fourier transform infrared spectroscopy (FTIR) and a flash EA 1112 elemental analyzer were used for confirming the graft process. The concentrations of F^- were measured using a PFS-80 fluoride analyzer. The concentrations of arsenic were measured using an AFS-9130 atomic fluorescence spectrophotometer.

3. Results and discussion

3.1. Synthesis of cellulose-g-PDMAEMA

The cellulose fibers have been fabricated just by mechanically grinding. The morphology of the obtained cellulose fibers is shown in Fig. 1a. Most of the cellulose fibers are 10–20 μm in diameter. Fig. 1b is the SEM image of the cellulose fibers after being grafted with PDMAEMA. As the grafting process on cellulose fiber surface is a heterogeneous reaction, the morphology and diameter of the fibers have not changed after grafting. Seen from the insets of Fig. 1, still no significant changes can be observed before and after surface modification, indicating that the heterogeneous grafting process will not change the features of cellulose fiber surface. Fig. 2 shows the FTIR spectra of cellulose fibers and the synthesized cellulose-g-PDMAEMA. The broad band around 3410 cm^{-1} is attributed to hydrogen bonding from –OH of cellulose. The band at 2901 cm^{-1} corresponds to the C–H stretching vibration, and the band at 1637 cm^{-1} represents H_2O that was adsorbed on the material surface. The absorption bands at 1431 cm^{-1}, 1165 cm^{-1}, 1115 cm^{-1} and 900 cm^{-1} are all the characteristic absorption bands of cellulose. These bands are assigned to CH_2 of pyran ring symmetric scissoring (1431 cm^{-1}), glucosidic bond asymmetry stretching (1165 cm^{-1}), the crystal absorption peak of cellulose I (1115 cm^{-1}),

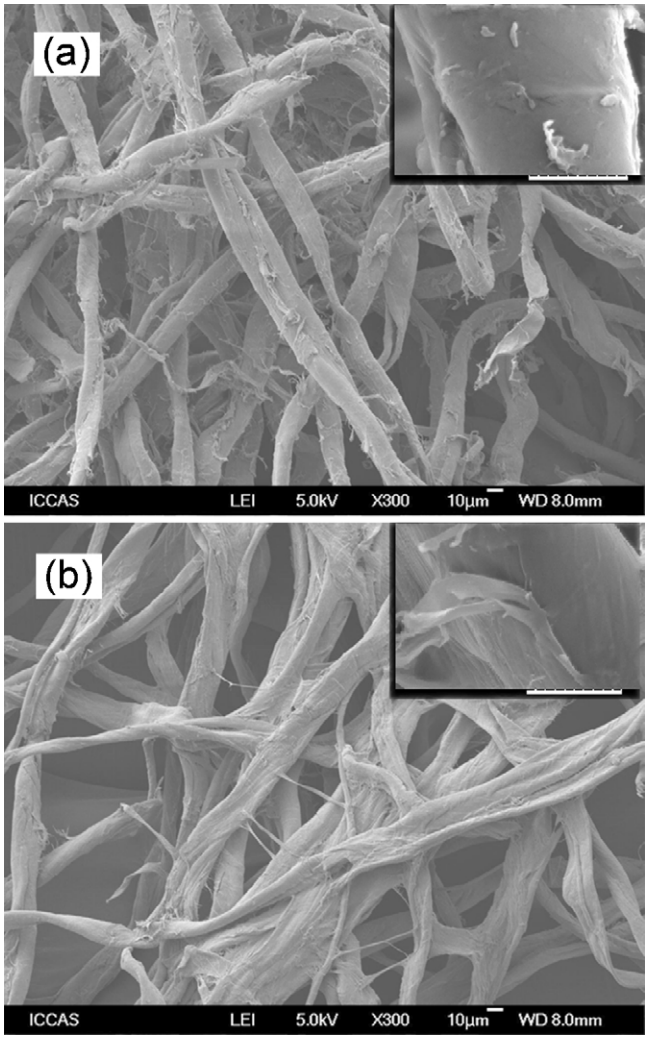

Fig. 1. SEM images of cellulose fibers before (a) and after (b) being grafted with PDMAEMA. The insets are SEM images of higher magnification to show the features on fiber surface (scale bar 5 μm).

and C–H out of plane stretching due to β-linkage (900 cm^{-1}), respectively. After the graft polymerization, these characteristic absorption bands of cellulose have not shifted at all, indicating the grafting reaction has not destroyed the basic molecular structure of cellulose. The characteristic absorption band of PDMAEMA that belongs to –COO– vibration appears at 1732 cm^{-1} in the spectrum of cellulose-g-PDMAEMA, and this proves evidence for the grafting of PDMAEMA onto cellulose. Table 1 shows the nitrogen content of the non-grafted and grafted cellulose obtained from elemental analysis method. There is little nitrogen in cellulose fibers (<0.30 wt%), while after grafting, an obvious increase in nitrogen content can be observed, which corresponds to the introduction of tertiary amine groups. So, the elemental analysis results also confirm the success of grafting. The content of tertiary amine groups and the grafted PDMAEMA can be calculated from the nitrogen content, shown in Table 1. The graft content can also be calculated by weighting estimation as follows: graft content = $[(W_g - W_0)/W_0] \times 100\%$, where W_g and W_0 are the weights of cellulose-g-PDMAEMA and cellulose fibers, respectively. By this way, the graft content of the synthesized fibers is around 11.20 wt%. And this value is close to the graft content calculated from the elemental analysis in Table 1.

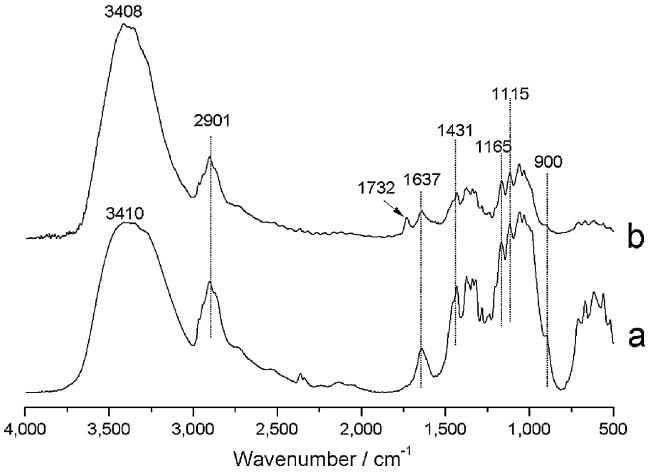

Fig. 2. FTIR spectra of cellulose fibers before (a) and after (b) being grafted with PDMAEMA.

Table 1
The content of N in cellulose fibers and synthesized cellulose-g-PDMAEMA, obtained from elemental analysis. The calculated content of tertiary amine groups and the grafted PDMAEMA was also included.

	Cellulose	Cellulose-g-PDMAEMA
Content of N (wt%)	<0.30	1.17
Content of tertiary amine groups (mmol/g)	–	0.836
Content of the grafted PDMAEMA (wt%)	–	13.1

3.2. Effect of initial concentrations and time on adsorption behaviors

Fig. 3 shows the adsorption behaviors of cellulose-g-PDMAEMA for F^-, AsO_2^- and AsO_4^{3-} at different initial ion concentrations, with the adsorbent dose being 1 g L^{-1}. In Fig. 3, the equilibrium adsorption capacity (q_e) for F^- increases with the initial F^- concentration (C_0). The q_e increases from 1.5 mg g^{-1} to 7.5 mg g^{-1} while the C_0 from 1.8 mg L^{-1} to 12.8 mg L^{-1}. This adsorption capacity is much higher compared to other adsorbents. For example, S. Meenakshi and co-workers [19] used protonated chitosan beads for F^- adsorption, and the q_e are 2.183–3.369 mg g^{-1} with C_0 from 11 mg L^{-1} to 17 mg L^{-1}. Their q_e is much lower and initial concentration is higher than ours. From the inset figure, we can find that when C_0 is below 4.5 mg L^{-1}, the F^- equilibrium concentration after adsorption process (C_e) can fit the WHO requirements of no higher than 1 mg L^{-1}. For C_0 higher than 4.5 mg L^{-1}, the WHO requirements can be achieved by increasing the adsorbent dose. Like F^- adsorption, q_e for As (III) and As (V) also increases with C_0 in the adsorption process. When the C_0 increases from 0.05 mg L^{-1} to 8.9 mg L^{-1}, the q_e rises up from 0.06 mg g^{-1} to 7.8 mg g^{-1} for As (III) and from 0.05 mg g^{-1} to 8.7 mg g^{-1} for As (V). The higher adsorption capacity for As (V) than As (III) is due to the more mobility of As (III) [33]. This difference can also be seen in the inset figures. For As (III), when C_0 exceeds 2.5 mg L^{-1}, the equilibrium concentration C_e will surpass the WHO guidline of 0.01 mg L^{-1}. And for As(V), a solution with C_0 below 5 mg L^{-1} can be treated to fit the WHO requirement. These results suggest that cellulose-g-PDMAEMA adsorbent is effective in the removal of F^-, AsO_2^- and AsO_4^{3-} from aqueous solutions, even at low initial concentrations.

Fig. 4 shows the effect of time on adsorption behaviors of cellulose-g-PDMAEMA for F^-, the adsorbent dose being 1 g L^{-1}. It is found that it has very quick adsorption kinetics. Within 1 min, the concentration of F^- reached equilibrium below 1 mg L^{-1}, and the removal efficiency reached above 86%. So, this adsorbent can efficiently adsorb anions in a very short cycle.

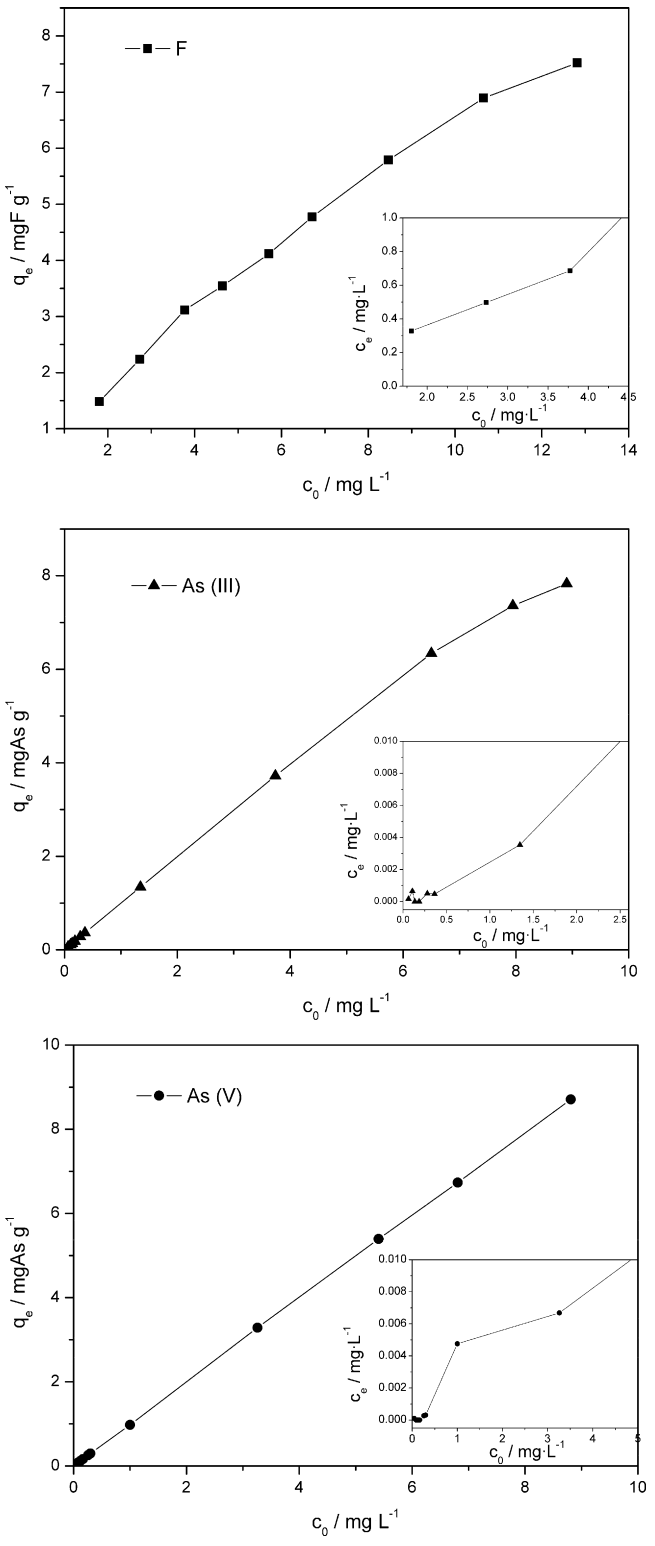

Fig. 3. Effect of initial concentrations on adsorption behaviors of cellulose-g-PDMAEMA for F^-, AsO_2^- and AsO_4^{3-} (adsorbent dose 1 g L^{-1}).

3.3. Distribution coefficient and competitive adsorption

The distribution coefficient K_D describes the binding ability of adsorbent surface to an element. K_D is a ratio of the element concentration in solid state and in water state, and it can be calculated

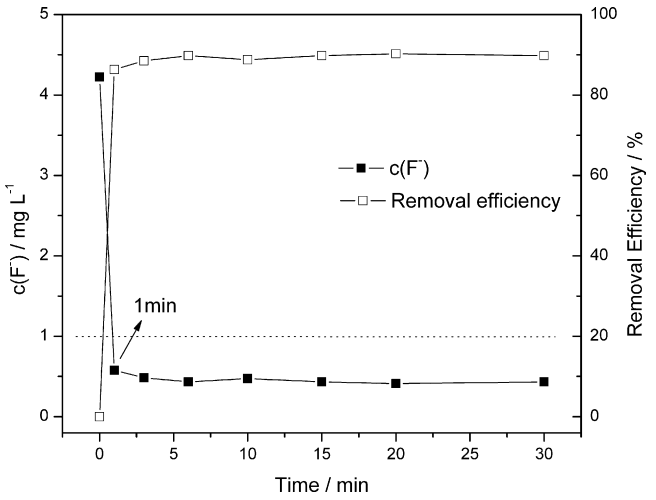

Fig. 4. The adsorption kinetics of cellulose-g-PDMAEMA for F^- (adsorbent dose 1 g L^{-1}).

from the following expression:

$$K_D = \frac{C_s}{C_w} \quad (2)$$

where C_s (mg g^{-1}) and C_w (mg L^{-1}) are the element concentrations in solid adsorbents and in water, respectively. And their values equal to the equilibrium adsorption capacity (q_e) and the equilibrium concentration (C_e), respectively. In real life water, there coexist many other anions such as Cl^-, SO_4^{2-} and HCO_3^-, which would compete with F^-, AsO_2^- and AsO_4^{3-} for the adsorption sites on the adsorbent surface. Fig. 5 shows distribution coefficient K_D of the adsorbent for F^-, AsO_2^-, AsO_4^{3-} and the competitive anions Cl^-, SO_4^{2-} and HCO_3^- with initial ion concentrations of 10 mg L^{-1}. A higher K_D value corresponds to higher binding ability to this anion. From Fig. 5 results, it can be found that the adsorption of these anions is selective to be in the order of $AsO_4^{3-} \gg AsO_2^- > SO_4^{2-} > F^- > Cl^- > HCO_3^-$. So, arsenic has extremely high binding ability on the adsorbent surface, and the adsorption behavior should not be influenced too much when competing anions coexist. For fluoride, the binding ability is comparatively low, and the adsorption for it may be influenced by other anions. Table 2 shows the fluoride and arsenic removal proportions without and with the competing anions. The composition of the mixed solutions is F^-, 2; AsO_2^- or AsO_4^{3-}, 1; Cl^-, 20; HCO_3^-, 20;

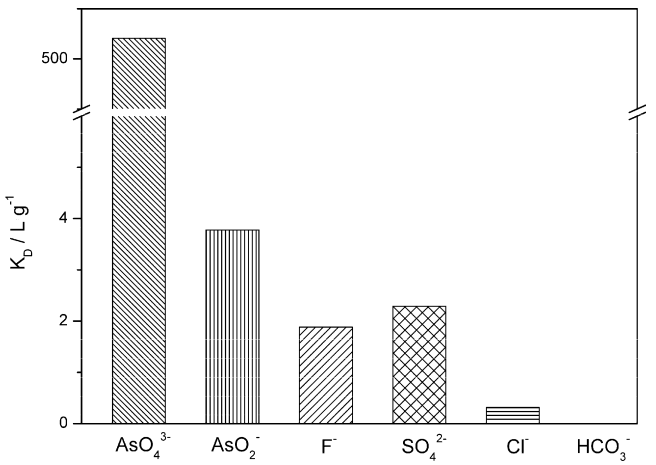

Fig. 5. K_D values of the adsorbent for AsO_4^{3-}, AsO_2^-, F^-, Cl^-, SO_4^{2-} and HCO_3^- with initial ion concentrations of 10 mg L^{-1}.

Table 2
The F and As removal proportions of the surface modified cellulose fibers with and without the competing anions, the composition of the mixed solution is F^-, 2; AsO_2^- or AsO_4^{3-}, 1; Cl^-, 20; HCO_3^-, 20; SO_4^{2-}, 20 mg L^{-1}.

Valence state of As	F^- Removal proportion		As removal proportion	
	Without competing anions	With competing anions	Without competing anions	With competing anions
III	81.81%	27.56%	99.74%	99.05%
V	81.81%	27.56%	99.56%	99.41%

SO_4^{2-}, 20 mg L^{-1}. It is noteworthy that F^-, and AsO_2^- or AsO_4^{3-} anions are coexistent here. The concentrations of the Cl^-, HCO_3^- and SO_4^{2-} in the mixed solutions (20 mg L^{-1}) are much higher than F^- (2 mg L^{-1}) and AsO_2^- or AsO_4^{3-} (1 mg L^{-1}). While the competing anions exist, the F^- removal proportions decreased from 81.81% to 27.56%, and the As removal proportions remain still above 99%. This suggests that in practical use for water treatment, we should increase the adsorbent dose for F^- removal, and we can totally ignore the influence of other anions on As removal.

According to the property of the adsorbent surface, the value of K_D for an element shows two different situations at a given pH value: if the surface is homogeneous, the K_D value stays the same with adsorbent dose, whereas if the surface is heterogeneous, the K_D value will increase with the adsorbent dose [34]. Fig. 6 shows the plot of K_D values of F^- as a function of adsorbent dose. It is found that as the adsorbent dose increased from 1 to 3 g L^{-1}, the distribution coefficient K_D stayed around 5 L g^{-1}, which implies that the surface of cellulose-g-PDMAEMA is homogeneous. That means the molecular chains of PDMAEMA, which are chemically bonded onto the cellulose fibers, should be totally dissolved into water. Based on this fact, this cellulose-g-PDMAEMA adsorbent has an attractive structure. For one thing, it has an insoluble fiber template that can be easily removed from water after the adsorption process. For another thing, its surface is covered with soluble PDMAEMA chains that have adsorptive sites on it.

This special structure of the adsorbent can explain the phenomena in Fig. 3. For heterogeneous adsorbent such as alumina [21] and zirconium-impregnated collagen [35], some of them are efficient only at high ion concentrations [27]. But for this cellulose-g-PDMAEMA, at low concentrations, the dissolved PDMAEMA chains on the surface have much more chances to contact with the harmful anions, so it is still effective and can decrease the ion concentrations down to the WHO level. The homogeneous surface can also explain the fast adsorption kinetics in Fig. 4. The adsorption process of anions can be divided into two processes, which are diffusion in water and surface reaction. Both of them happen homogeneously, so the adsorption process will be very fast. And this is quite helpful in practical use.

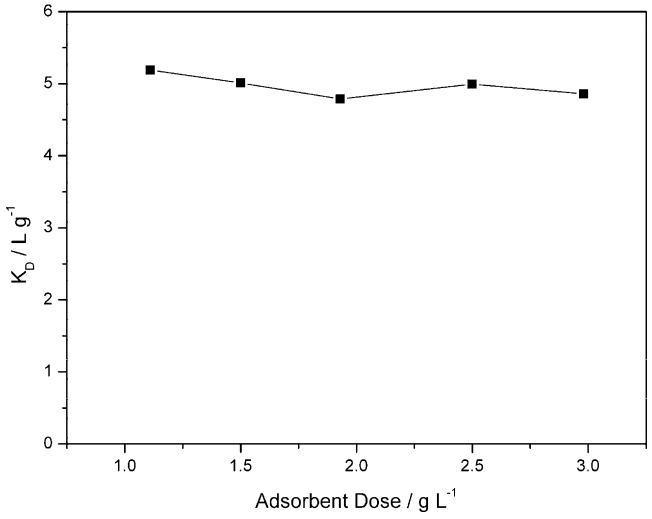

Fig. 6. Plot of K_D values of F^- as a function of adsorbent dose.

3.4. Effect of pH values on adsorption behaviors

Fig. 7 shows the effect of initial pH values on the adsorption behaviors, with the adsorbent dose keeping 1 g L^{-1}. It is found that at pH < 10, the adsorbent keeps high q_e. While at higher pH (pH > 10), the q_e decreases sharply with increasing pH value, even decreases to zero for F^-. This adsorption behavior is attributed to the pH-responsibility of PDMAEMA. On this adsorbent surface, it is the tertiary amine group ($-NR_1R_2$) on the PDMAEMA chains that is responsible for the binding of anions. The solubility and the charged properties of the grafted PDMAEMA polymer chains are both pH-responsive [36,37]. At lower pH, the tertiary amine group $-NR_1R_2$ can be protonated to $-NR_1R_2H^+$, and the electric repulsion between $-NR_1R_2H^+$ can overcome the tendency of the chains to collapse or aggregate in water. While at higher pH, the tertiary amine group is deprotonated to $-NR_1R_2$ and the uncharged chains will collapse or aggregate. So the grafted PDMAEMA will become positive-charged and totally dissolved chains at lower pH and become uncharged and collapsed chains at higher pH. (See Fig. 7) As a result, lower pH can raise the chance for the adsorptive sites to contact and adsorb harmful anions in water, and enhance the adsorption capacity of cellulose-g-PDMAEMA. Furthermore, the arsenic chemistry in water is highly dependent on pH, too [38]. For As(III), at pH < 9.2, the uncharged species $H_3AsO_3^0$ will predominate in water, so the q_e for As(III) will also decrease with the decreasing of pH, leaving the highest q_e at pH ≈ 9. For As(V), the pH range for uncharged species $H_3AsO_4^0$ predominating in water is very narrow (pH < 2), so the q_e will not change a lot at lower pH. Similar phenomena have

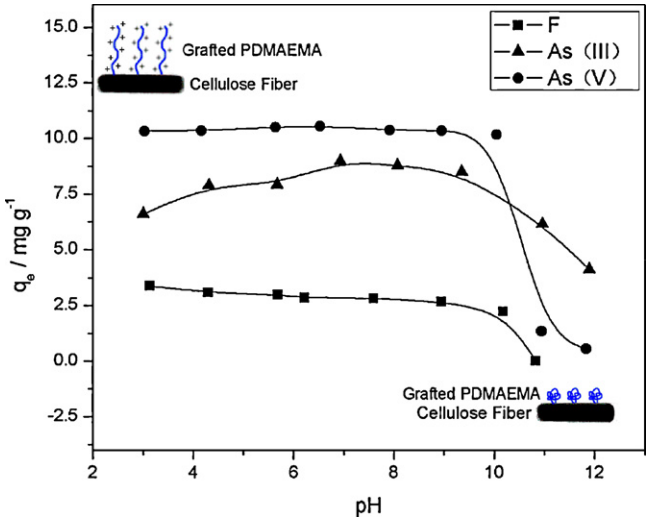

Fig. 7. Effect of initial pH values on adsorption capacities of cellulose-g-PDMAEMA for F^-, As(III) and As(V), adsorbent dose: 1 g L^{-1}, initial concentrations: 4 mg L^{-1} for F^-, 10 mg L^{-1} for As(III) and As(V).

Table 3
Langmuir, Freundlich and Temkin parameters for adsorption isotherms of cellulose-g-PDMAEMA at 30 °C. The r^2 values correspond to the linear correlation coefficients.

	Langmuir parameters		
	Q_0 (mg g^{-1})	b (L mg^{-1})	r^2
F^-	8.59	1.06	0.979
As(III)	8.96	16.63	0.995
As(V)	27.93	27.76	0.940
	Freundlich parameters		
	K_f (mg g^{-1})	n	r^2
F^-	4.23	2.83	0.994
As(III)	8.46	3.78	0.838
As(V)	350.55	1.13	0.992
	Temkin parameters		
	A_T (L mg^{-1})	b_T (J mol^{-1})	r^2
F^-	14.6	1504	0.972
As(III)	1430	2255	0.968
As(V)	845	840	0.934

been reported for arsenic adsorption on nanocrystalline titanium dioxide [39].

3.5. Adsorption isotherms

Adsorption isotherms are useful to determine the amount of adsorbent needed to adsorb a required amount of adsorbate. In the present study, the equilibrium condition was kept at 30 °C, and the adsorption isotherms were analyzed by the three most commonly used model equations, which were Langmuir, Freundlich and Temkin (see Fig. 8). The parameters calculated from the three models were stated in Table 3.

The Langmuir isotherm model [40], which assumes monolayer adsorption with uniform energies of adsorption on the surface, can be expressed as Eq. (3):

$$\frac{C_e}{q_e} = \frac{1}{Q_0 b} + \frac{C_e}{Q_0} \quad (3)$$

where C_e (mg L^{-1}) and q_e (mg g^{-1}) are the concentration and adsorption capacity at equilibrium, respectively. Q_0 (mg g^{-1}) and b (L mg^{-1}) are Langmuir constants related to maximum adsorption capacity and adsorption energy, respectively. From the values of Q_0 in Table 3, we can see that the maximum adsorption capacity for the three kind of anions are in the order of: As(V) ≫ As(III) > F^-. In Langmuir model, a dimensionless parameter called separation factor (R_L) [41] can be defined as:

$$R_L = \frac{1}{1 + bC_0} \quad (4)$$

In the initial ion concentration (C_0) range of our study, the values are all $0 < R_L < 1$, indicating the adsorption process is favorable.

The Freundlich model [42] is based on a multilayer adsorption with the adsorption energy decreasing with the surface coverage. It is expressed as Eq. (5):

$$\ln q_e = \ln K_f + \frac{1}{n} \ln C_e \quad (5)$$

where q_e and C_e are the same meaning as noted previously. K_f (mg g^{-1}) and n are Freundlich constants measuring the adsorption capacity and the adsorption intensity, relatively. The K_f value for F^-, As(III) and As(V) is 4.23 mg g^{-1}, 8.46 mg g^{-1} and 350.55 mg g^{-1}, respectively, suggesting that the anion binding affinity on cellulose-g-PDMAEMA can be in the order of As(V) ≫ As(III) > F^-. The n values for F^-, As(III) and As(V) are all $1 < n < 10$, indicating that adsorption is a favorable process.

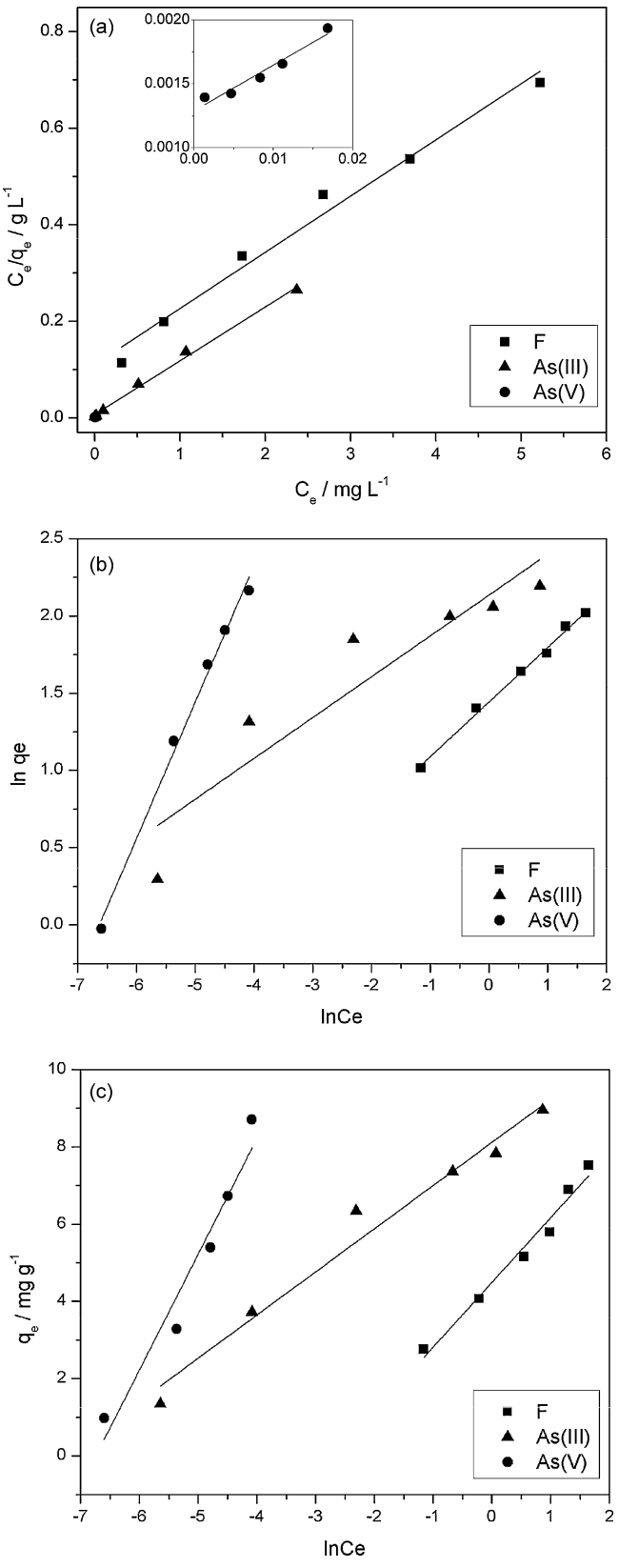

Fig. 8. Linear plots of adsorption isotherms at 30 °C fitting by (a) Langmuir, (b) Freundlich and (c) Temkin models.

Table 4
Comparison of the Langmuir capacity of different adsorbents for fluoride and arsenic adsorption.

Adsorbent	Q_0 (mg g^{-1})			Reference
	F^-	As(III)	As(V)	
Chitosan beads	7.32	–	–	[19]
Laterite	0.846	–	–	[44]
Manganese-oxide-coated alumina	2.851	–	–	[45]
Iron hydroxide-coated alumina	–	7.65	15.9	[46]
Cupric oxide nanoparticles	–	26.9	22.6	[47]
Ce-Ti oxide adsorbent	–	–	45.0	[48]
Cellulose-g-PDMAEMA	8.59	8.96	27.93	This study

Temkin isotherm [43] assumes that the fall in the heat of adsorption is linear rather than logarithmic, as implied in the Freundlich equation. It can be applied in Eq. (6):

$$q_e = \frac{RT}{b_T} \ln A_T + \frac{RT}{b_T} \ln C_e \quad (6)$$

where q_e and C_e are the same meaning as noted previously, and A_T (L mg^{-1}) and b_T (J mol^{-1}) are the Temkin constants. R is the universal gas constant 8.314 J mol^{-1} K^{-1} and T is the absolute temperature 303 K. Based on the linear correlation coefficients, r^2 in Table 3, the fitness of the three models is in the order of Langmuir (r^2 = 0.940–0.995) > Temkin (r^2 = 0.934–0.972) > Freundlich (r^2 = 0.838–0.994). It indicates that the adsorption isotherms of F^-, AsO_2^- and AsO_4^{3-} onto cellulose-g-PDMAEMA fit Langmuir model a little better than Freundlich and Temkin models. The Langmuir capacity for fluoride and arsenic of different adsorbents is given in Table 4. By comparison, it can be stated that the adsorption capacity of our adsorbent is competitive. In addition, the cellulose-g-PDMAEMA can adsorb both arsenic and fluoride in high efficiency, and this is the main advantage that other adsorbents do not possess.

4. Conclusions

Cellulose-g-PDMAEMA adsorbent for F^-, AsO_2^- and AsO_4^{3-} has been fabricated successfully by modifying the surface of native cellulose fibers with poly(*N*,*N*-dimethyl aminoethyl methacrylate) (PDMAEMA). This adsorbent has an insoluble cellulose template but soluble PDMAEMA grafted polymer chains on the surface. So it has a homogeneous adsorption process, in which the distribution coefficient will not change with adsorbent dose. Based on the homogeneous adsorption feature, it has quite fast adsorption kinetics (reaching equilibrium within 1 min), and it is still effective at very low initial concentrations. PH value influences the adsorption characteristics because of the pH-responsibility of PDMAEMA. Other anions such as Cl^-, HCO_3^- and SO_4^{2-} can hardly affect arsenic adsorption of the adsorbent but will compete with F^- and reduce the F^- removal proportion. The Langmuir, Freundlich and Temkin isotherm models are introduced to interpret the experimental data. The results show Langmuir model fits best for the three anions. The adsorption capacities calculated from Langmuir and Freundlich equations are both in the order of $AsO_4^{3-} \gg AsO_2^- > F^-$. The values of separation factor (R_L) and Freundlich constant n show that the adsorption is a favorable process. This work gives useful information to prepare adsorbents with high efficiency using agro- or plant-residues.

Acknowledgements

This work was supported by National Natural Scientific Foundation of China (No. 50773086, 50821062) and National Program on Key Basic Research Project (973 Program, No. 2011CB933700).

References

[1] C. Zhu, G. Bai, X. Liu, Y. Li, Screening high-fluoride and high-arsenic drinking waters and surveying endemic fluorosis and arsenism in Shaanxi province in western China, Water Res. 40 (2006) 3015–3022.
[2] P. Bagla, J. Kaiser, Epidemiology – India's spreading health crisis draws global arsenic experts, Science 274 (1996) 174–175.
[3] K. Thornburg, N. Sahai, Arsenic occurrence, mobility, and 14 retardation in sandstone and dolomite formations of the Fox River Valley, eastern Wisconsin, Environ. Sci. Technol. 38 (2004) 5087–5094.
[4] J.A. Nell, G. Livanos, Effects of fluoride concentration in seawater on growth and fluoride accumulation by sydney rock oyster (saccostrea-commercials) and flat oyster (oyster-angasi) spat, Water Res. 22 (1988) 749–753.
[5] W.E. Brown, T.M. Gregory, L.C. Chow, Effects of fluoride on enamel solubility and cariostasis, Caries Res. 11 (1977) 118–136.
[6] K. Banerjee, G.L. Amy, M. Prevost, S. Nour, M. Jekel, P.M. Gallagher, C.D. Blumenschein, Kinetic and thermodynamic aspects of adsorption of arsenic onto granular ferric hydroxide (GFH), Water Res. 42 (2008) 3371–3378.
[7] A.H. Smith, C. Hopenhaynrich, M.N. Bates, H.M. Goeden, I. Hertzpicciotto, H.M. Duggan, R. Wood, M.J. Kosnett, M.T. Smith, Cancer risks from arsenic in drinking-water, Environ. Health Perspect. 97 (1992) 259–267.
[8] WHO, Guidelines for drinking water quality, World Health Organization, Geneva, Switzerland, 1993.
[9] J. Camacho, H.-Y. Wee, T.A. Kramer, R. Autenrieth, Arsenic stabilization on water treatment residuals by calcium addition, J. Hazard. Mater. 165 (2009) 599–603.
[10] B.D. Turner, P. Binning, S.L.S. Stipp, Fluoride removal by calcite: evidence for fluorite precipitation and surface adsorption, Environ. Sci. Technol. 39 (2005) 9561–9568.
[11] T. Ishihara, Y. Misumi, H. Matsumoto, Pore size control for mesoporous titanium hydroxide prepared with mixed template molecules and its fluoride ion-exchange property, Microporous Mesoporous Mater. 122 (2009) 87–92.
[12] J. Kim, M.M. Benjamin, Modeling a novel ion exchange process for arsenic and nitrate removal, Water Res. 38 (2004) 2053–2062.
[13] B.A. Manning, S.E. Fendorf, B. Bostick, D.L. Suarez, Arsenic(III) oxidation and arsenic(V) adsorption reactions on synthetic birnessite, Environ. Sci. Technol. 36 (2002) 976–981.
[14] A. Tor, Removal of fluoride from water using anion-exchange membrane under Donnan dialysis condition, J. Hazard. Mater. 141 (2007) 814–818.
[15] J.W. Wang, D. Bejan, N.J. Bunce, Removal of arsenic from synthetic acid mine drainage by electrochemical pH adjustment and coprecipitation with iron hydroxide, Environ. Sci. Technol. 37 (2003) 4500–4506.
[16] C.Y. Hu, S.L. Lo, W.H. Kuan, Effects of the molar ratio of hydroxide and fluoride to Al(III) on fluoride removal by coagulation and electrocoagulation, J. Colloid Interface Sci. 283 (2005) 472–476.
[17] G.T. Schmidt, K.H. Lui, M. Kersten, Speciation and mobility of arsenic in agricultural lime, J. Environ. Qual. 38 (2009) 2058–2069.
[18] M. Jang, W. Chen, F.S. Cannon, Preloading hydrous ferric oxide into granular activated carbon for arsenic removal, Environ. Sci. Technol. 42 (2008) 3369–3374.
[19] N. Viswanathan, C.S. Sundaram, S. Meenakshi, Removal of fluoride from aqueous solution using protonated chitosan beads, J. Hazard. Mater. 161 (2009) 423–430.
[20] V.M. Boddu, K. Abburi, J.L. Talbott, E.D. Smith, R. Haasch, Removal of arsenic(III) and arsenic(V) from aqueous medium using chitosan-coated biosorbent, Water Res. 42 (2008) 633–642.
[21] Y. Kim, C. Kim, I. Choi, S. Rengaraj, J. Yi, Arsenic removal using mesoporous alumina prepared via a templating method, Environ. Sci. Technol. 38 (2003) 924–931.
[22] M. Yang, T. Hashimoto, N. Hoshi, H. Myoga, Fluoride removal in a fixed bed packed with granular calcite, Water Res. 33 (1999) 3395–3402.
[23] R. Piekos, S. Paslawska, Fluoride uptake characteristics of fly ash, in: XXIInd Conference of the International-Society-for-Fluoride-Research, Int Soc Fluoride Research, Bellingham, Washington, 1998, pp. 14–19.
[24] S.A. Wasay, J. Haron, S. Tokunaga, Adsorption of fluoride, phosphate, and arsenate ions on lanthanum impregnated silica gel, Water Environ. Res. 68 (1996) 295–300.
[25] Y.N. Chen, L.Y. Chai, Y.D. Shu, Study of arsenic(V) adsorption on bone char from aqueous solution, J. Hazard. Mater. 160 (2008) 168–172.
[26] N.A. Medellin-Castillo, R. Leyva-Ramos, R. Ocampo-Perez, R.F.G. de la Cruz, A. Aragon-Pina, J.M. Martinez-Rosales, R.M. Guerrero-Coronado, L. Fuentes-Rubio, Adsorption of fluoride from water solution on bone char, Ind. Eng. Chem. Res. 46 (2007) 9205–9212.
[27] X. Fan, D.J. Parker, M.D. Smith, Adsorption kinetics of fluoride on low cost materials, Water Res. 37 (2003) 4929–4937.
[28] B.L. Rivas, M.d.C. Aguirre, E. Pereira, C. Bucher, G. Royal, D. Limosin, E.S. Aman, J.-C. Moutet, Off-line coupled electrocatalytic oxidation and liquid phase polymer based retention (EO-LPR) techniques to remove arsenic from aqueous solutions, Water Res. 43 (2009) 515–521.
[29] Z.B. Zhang, X.L. Zhu, F.J. Xu, K.G. Neoh, E.T. Kang, Temperature- and pH-sensitive nylon membranes prepared via consecutive surface-initiated atom transfer radical graft polymerizations, J. Membr. Sci. 342 (2009) 300–306.
[30] N.A. Hadjiantoniou, T. Krasia-Christoforou, E. Loizou, L. Porcar, C.S. Patrickios, Alternating amphiphilic multiblock copolymers: controlled synthesis via RAFT polymerization and aqueous solution characterization, Macromolecules 43 (2010) 2713–2720.

[31] K.C. Gupta, S. Sahoo, Graft copolymerization of acrylonitrile and ethyl methacrylate comonomers on cellulose using ceric ions, Biomacromolecules 2 (2001) 239–247.
[32] K.C. Gupta, K. Khandekar, Temperature-responsive cellulose by ceric(IV) ion-initiated graft copolymerization of N-isopropylacrylamide, Biomacromolecules 4 (2003) 758–765.
[33] J.F. Ferguson, J. Gavis, Review of arsenic cycle in natural waters, Water Res. 6 (1972) 1259–1274.
[34] D.P. Das, J. Das, K. Parida, Physicochemical characterization and adsorption behavior of calcined Zn/Al hydrotalcite-like compound (HTlc) towards removal of fluoride from aqueous solution, J. Colloid Interface Sci. 261 (2003) 213–220.
[35] X.-p. Liao, B. Shi, Adsorption of fluoride on zirconium(IV)-impregnated collagen fiber, Environ. Sci. Technol. 39 (2005) 4628–4632.
[36] W. Zhang, J. He, Z. Liu, P. Ni, X. Zhu, Biocompatible and pH-responsive triblock copolymer mPEG-b-PCL-b-PDMAEMA: synthesis, self-assembly, and application, J. Polym. Sci., Part A: Polym. Chem. 48 (2010) 1079–1091.
[37] N. Karanikolopoulos, M. Zamurovic, M. Pitsikalis, N. Hadjichristidis, Poly(dl-lactide)-b-poly(*N*,*N*-dimethylamino-2-ethyl methacrylate): synthesis, characterization, micellization behavior in aqueous solutions, and encapsulation of the hydrophobic drug dipyridamole, Biomacromolecules 11 (2009) 430–438.
[38] P.L Smedley, D.G. Kinniburgh, A review of the source, behaviour and distribution of arsenic in natural waters, Appl. Geochem. 17 (2002) 517–568.
[39] M. Pena, X. Meng, G.P. Korfiatis, C. Jing, Adsorption mechanism of arsenic on nanocrystalline titanium dioxide, Environ. Sci. Technol. 40 (2006) 1257–1262.
[40] I. Langmuir, The adsorption of gases on plane surfaces of glass, mica and platinum, J. Am. Chem. Soc. 40 (1918) 1361–1403.
[41] F. Deniz, S.D. Saygideger, Equilibrium, kinetic and thermodynamic studies of Acid Orange 52 dye biosorption by Paulownia tomentosa Steud. leaf powder as a low-cost natural biosorbent, Bioresour. Technol. 101 (2010) 5137–5143.
[42] H. Freundlich, Concerning adsorption in solutions, Z. Phys. Chem. – Stochiometrie Und Verwandtschaftslehre 57 (1906) 385–470.
[43] M. Temkin, V. Pyzhev, Kinetics of ammonia synthesis on promoted iron catalysts, Acta Physicochim. Urss 12 (1940) 327–356.
[44] M. Sarkar, A. Banerjee, P.P. Pramanick, A.R. Sarkar, Use of laterite for the removal of fluoride from contaminated drinking water, J. Colloid Interface Sci. 302 (2006) 432–441.
[45] S.M. Maliyekkal, A.K. Sharma, L. Philip, Manganese-oxide-coated alumina: a promising sorbent for defluoridation of water, Water Res. 40 (2006) 3497–3506.
[46] J. Hlavay, K. Polyak, Determination of surface properties of iron hydroxide-coated alumina adsorbent prepared for removal of arsenic from drinking water, J. Colloid Interface Sci. 284 (2005) 71–77.
[47] C.A. Martinson, K.J. Reddy, Adsorption of arsenic(III) and arsenic(V) by cupric oxide nanoparticles, J. Colloid Interface Sci. 336 (2009) 406–411.
[48] S.B. Deng, Z.J. Li, J. Huang, G. Yu, Preparation, characterization and application of a Ce-Ti oxide adsorbent for enhanced removal of arsenate from water, J. Hazard. Mater. 179 (2010) 1014–1021.